Published OnlineFirst June 9, 2009; DOI: 10.1158/1535-7163.MCT-08-1208

Preclinical evaluation of a novel pyrimidopyrimidine for the prevention of nucleoside and nucleobase reversal of antifolate cytotoxicity

Huw D. Thomas,[1] Kappusamy Saravanan,[2] Lan-Zhen Wang,[1] Mei-Ju Lin,[1] Julian S. Northen,[2] Hannah Barlow,[2] Marion Barton,[2] David R. Newell,[1] Roger J. Griffin,[2] Bernard T. Golding,[2] and Nicola J. Curtin[1]

[1]Northern Institute for Cancer Research, Medical School, and [2]Northern Institute for Cancer Research, School of Chemistry, Newcastle University, Newcastle upon Tyne, United Kingdom

Abstract

Antifolates have been used to treat cancer for the last 50 years and remain the mainstay of many therapeutic regimes. Nucleoside salvage, which depends on plasma membrane transport, can compromise the activity of antifolates. The cardiovascular drug dipyridamole inhibits nucleoside transport and enhances antifolate cytotoxicity *in vitro*, but its clinical activity is compromised by binding to the plasma protein α_1-acid glycoprotein (AGP). We report the development of a novel pyrimidopyrimidine analogue of dipyridamole, NU3153, which has equivalent potency to dipyridamole, remains active in the presence of physiologic levels of AGP, inhibits thymidine incorporation into DNA, and prevents thymidine and hypoxanthine rescue from the multitargeted antifolate, pemetrexed. Pharmacokinetic evaluation of NU3153 suggested that a soluble prodrug would improve the *in vivo* activity. The valine prodrug of NU3153, NU3166, rapidly broke down to NU3153 *in vitro* and *in vivo*. Plasma NU3153 concentrations commensurate with rescue inhibition *in vitro* were maintained for at least 16 hours following administration of NU3166 to mice at 120 mg/kg. However, maximum inhibition of thymidine incorporation into tumors was only 50%, which was insufficient to enhance pemetrexed antitumor activity *in vivo*. Comparison with the cell-based studies revealed that pemetrexed enhancement requires substantial (≥90%) and durable inhibition of nucleoside transport. In conclusion, we have developed non-AGP binding nucleoside transport inhibitors. Pharmacologically active concentrations of the inhibitors can be achieved *in vivo* using prodrug approaches, but greater potency is required to evaluate inhibition of nucleoside rescue as a therapeutic maneuver. [Mol Cancer Ther 2009;8 (7):1828–37]

Introduction

Antimetabolites were the first rationally designed anticancer drugs and still represent a major class with wide therapeutic applications today. In addition to methotrexate, several novel antifolates have been recently introduced to the clinic (reviewed in ref. 1). However, salvage of extracellular purine or pyrimidine nucleosides or bases constitutes an intrinsic resistance mechanism to antimetabolite inhibitors of *de novo* purine or pyrimidine biosynthesis. There is good evidence that the activities of salvage enzymes in cancer cells are higher than those of *de novo* synthesis (2). Furthermore, resistance to antimetabolites by virtue of the activity of salvage pathways increases in parallel with malignancy (3). More importantly, several preclinical studies show that nucleoside and nucleobase salvage by thymidine kinase (TK) and hypoxanthine-guanine phosphoribosyltransferase compromises the antitumor activity of antifolates. For example, the thymidylate synthase inhibitor AG337 was more active against xenografts deficient in TK than in tumors expressing this enzyme (4). Similarly, pemetrexed completely inhibited the growth of the TK-deficient and hypoxanthine-guanine phosphoribosyltransferase–deficient tumor (LY5178Y/TK^-/HX^-), but higher and longer dosing schedules were required to inhibit tumor growth in mice bearing wild-type LY5178Y tumors (5). Furthermore, whereas pemetrexed had only modest activity against parental GC3 xenografts at the maximum tolerated dose, it caused marked regressions of GC3 TK-deficient xenografts (6).

Nucleoside salvage is dependent on transport across the plasma membrane, with the principal route being carrier-mediated facilitated diffusion mediated by the widely distributed equilibrative transporters, ENT1 and ENT2, with broad selectivities, and the concentrative nucleoside transporters, CNT1, CNT2, and CNT3, which vary in their permeant selectivities and distribution (7). Hypoxanthine may enter via ENT2 or another thus far unidentified carrier. The pyrimidopyrimidine cardiovascular drug dipyridamole (Fig. 1) inhibits equilibrative nucleoside transporters (7, 8).

Received 12/22/08; revised 3/12/09; accepted 4/12/09; published OnlineFirst 6/9/09.

Grant support: Development Committee of Cancer Research UK. H.D. Thomas, L-Z. Wang, D.R. Newell, R.J. Griffin, and N.J. Curtin are funded by a Cancer Research UK program grant.

The costs of publication of this article were defrayed in part by the payment of page charges. This article must therefore be hereby marked *advertisement* in accordance with 18 U.S.C. Section 1734 solely to indicate this fact.

Requests for reprints: Nicola J. Curtin, Northern Institute for Cancer Research, Newcastle University, Paul O'Gorman Building, Newcastle upon Tyne NE2 4HH, United Kingdom. Phone: 44-191-246-4415; Fax: 44-191-246-4301. E-mail: n.j.curtin@ncl.ac.uk

doi:10.1158/1535-7163.MCT-08-1208

Published OnlineFirst June 9, 2009; DOI: 10.1158/1535-7163.MCT-08-1208

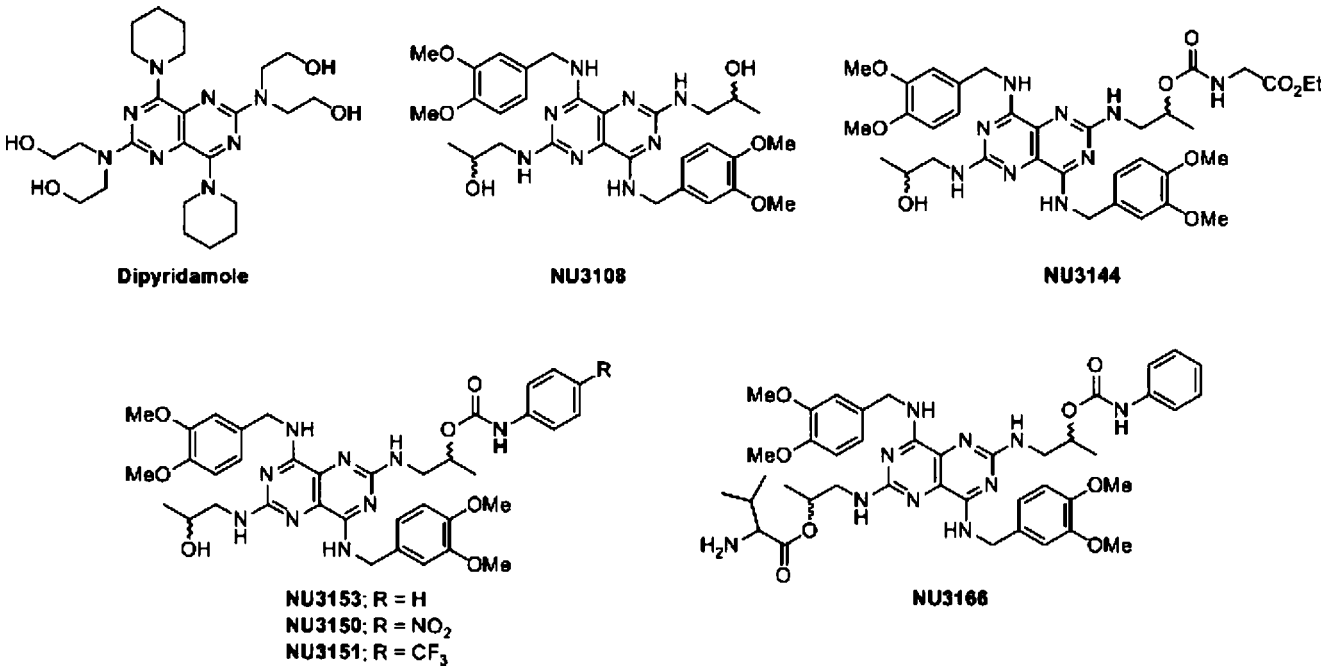

Figure 1. Structures of dipyridamole and novel pyrimidopyrimidine nucleoside transport inhibitors.

Several studies show that dipyridamole significantly increases the cytotoxic and antitumor activity of a variety of inhibitors of *de novo* nucleotide synthesis by blocking uptake of nucleosides for salvage (reviewed in ref. 9). Moreover, by blocking nucleoside efflux dipyridamole can also exacerbate antifolate-induced nucleotide pool imbalances and increase their cytotoxicities (10).

The promise of these preclinical studies, which showed the potential to enhance the efficacy of antimetabolites with dipyridamole, was not realized clinically. Lack of clinical efficacy was due in part to the avid binding of dipyridamole to the serum protein α_1-acid glycoprotein (AGP), which reduces the free dipyridamole levels to ineffective concentrations (11). In cancer patients, AGP levels are increased, thereby exacerbating the problem. In two clinical studies in which dipyridamole was administered, with the aim of increasing antimetabolite activity, the total plasma concentrations of dipyridamole were 12 and 16 μmol/L, but the free plasma concentrations were only 27 and 38 nmol/L, respectively (12, 13).

As part of a program to develop potent pyrimidopyrimidine analogues of dipyridamole with reduced AGP binding, we have optimized our initial lead compound, NU3076, a pyrimidopyrimidine that has comparable potency to dipyridamole without being affected by AGP (14). Several analogues that inhibit nucleoside transport even in the presence of physiologic concentrations of AGP were identified (15). Two of these analogues, NU3108 and NU3121, inhibited thymidine and hypoxanthine rescue from pemetrexed cytotoxicity in the presence and absence of AGP but, following the administration to mice at the maximum administrable dose, the plasma concentrations required for inhibition of thymidine incorporation, and hence rescue, into human tumor xenografts were only maintained for 2 hours (16). Our *in vitro* studies indicated that more prolonged and profound inhibition of thymidine incorporation was necessary for *in vivo* rescue inhibition. To overcome the restriction of the maximum administrable dose, due to the limited aqueous solubility of NU3108 and NU3121, we developed more soluble analogues. NU3144 (Fig. 1) was developed as a water-soluble prodrug of NU3108, based on a glycine carbamate, by hydrolyzing the ester to the carboxylic acid and formulating as a sodium salt. The observation that NU3144 was also more potent than the parent NU3108 prompted the synthesis of further arylcarbamates, including NU3150, NU3151, and NU3153 (Fig. 1).

We describe here the ability of all four compounds to inhibit thymidine uptake and prevent thymidine and hypoxanthine rescue from pemetrexed-induced growth inhibition *in vitro*. Based on these data, NU3153 and its water-soluble prodrug were taken into *in vivo* pharmacokinetic, pharmacodynamic, and efficacy studies.

Materials and Methods

Materials

All chemicals were from Sigma unless otherwise stated. Pemetrexed, a kind gift from Eli Lilly and Co., was dissolved in water. Thymidine, hypoxanthine, and dipyridamole were dissolved in water, 0.1 mol/L NaOH, and 100% DMSO, respectively. All solutions were stored in the dark at 4°C for a maximum of 4 wk. Novel nucleoside transport

Published OnlineFirst June 9, 2009; DOI: 10.1158/1535-7163.MCT-08-1208

inhibitors, synthesized at the Department of Chemistry, Northern Institute for Cancer Research, Newcastle University, unless otherwise indicated, were dissolved in DMSO and stored at −20°C (15). [^{3}H]Thymidine (37 MBq/mL, 1.78 TBq/mmol) and [^{14}C]sucrose (7.4 MBq/mL, 23.2 GBq/mmol) were obtained from Amersham International.

Cell Culture

COR-L23 lung cancer cells (a gift from the late Dr. P. Twentyman, MRC Clinical Oncology and Radiotherapeutics Unit, Cambridge, United Kingdom) and L1210 murine leukemia cells (European Collection of Animal Cell Cultures) were grown in RPMI 1640 supplemented with 1,000 units/mL penicillin, 100 μg/mL streptomycin (Life Technologies), and 10% (v/v) FCS. All cells were maintained as exponentially growing cultures and shown to be negative for *Mycoplasma* contamination (MycoAlert, Lonza).

Thymidine Transport Assays

We used a modified rapid mixing technique, combined with an inhibitor-stop method, to determine thymidine uptake into L1210 murine leukemia cells, as described previously (14, 17). Briefly, we suspended cells in transport buffer [130 mmol/L NaCl, 5 mmol/L KCl, 1 mmol/L $MgCl_2$, 5 mmol/L NaH_2PO_4, 10 mmol/L glucose, 10 mmol/L HEPES (pH 7.4)] in the presence and absence of inhibitor and/or AGP (5 mg/mL final concentration) and initiated transport by addition of [^{3}H]thymidine (final concentration = 100 μmol/L, 6.16 GBq/mmol, 617 KBq/mL) and [^{14}C]sucrose (2.13 μmol/L, 23.2 GBq/mmol, 49 KBq/mL) and terminated it at 2-s intervals by the addition of 100 μmol/L dipyridamole. Cells were then centrifuged through oil into a lysis solution of 3 mol/L KOH, neutralized with acetic acid, and counted by liquid scintillography on a Wallac 1410 liquid scintillation counter (Pharmacia Wallac). Cellular uptake was calculated by reference to 10 μL (3 nmol [^{3}H]thymidine-6.38 nmol [^{14}C]sucrose) of the radiolabel mixture. These standards were also used to calculate the [^{14}C]/[^{3}H] ratio and hence to determine the nontransported [^{3}H]thymidine in the extracellular space that was carried through the oil layer.

The percentage reduction in inhibitory potency of the compounds by AGP was calculated as follows: 100 − 100 × (% inhibition of thymidine uptake with AGP) / (% inhibition of thymidine uptake without AGP).

Thymidine Incorporation Assays

We measured incorporation of 100 nmol/L [^{3}H]thymidine into exponentially growing L1210 and COR-L23 cells over a period of 2 h in the presence or absence of inhibitors as described previously (18). Briefly, we seeded 2×10^4 COR-L23 cells per well in 96-well plates and allowed them to attach before washing with PBS and incubating with [^{3}H]thymidine (100 nmol/L specific activity, 6.2 GBq/mmol, 177.6 KBq/mL) in serum-free medium supplemented with 0.5% (v/v) DMSO with or without dipyridamole or novel inhibitors at 1 μmol/L for 2 h at 37°C. We washed the cells with ice-cold PBS and solubilized them with 0.5 mol/L NaOH before transfer to glass fiber filters (Flow Laboratories Ltd.) using the Titertek cell harvester apparatus (Flow Laboratories) rinsing with 10% (w/v) trichloroacetic acid, water, and methanol. After drying the filters, we measured the amount of [^{3}H]thymidine incorporated into DNA and retained on the filter by liquid scintillography by reference to a 10 pmol [^{3}H]thymidine (6.2 GBq/mmol) standard. We used a similar procedure for L1210 cells except that exponentially growing cells, washed with PBS, were seeded directly in 96-well plates at 2×10^4 per well in serum-free medium supplemented with 0.5% (v/v) DMSO with or without dipyridamole or novel inhibitors at 1 μmol/L, and the reactions were initiated by the addition of [^{3}H]thymidine (final concentration, 100 nmol/L; specific activity, 6.2 GBq/mmol). After 2 h of incubation at 37°C, the plates were centrifuged and washed gently twice with ice-cold PBS, with centrifugation between washes, before solubilization, harvesting, and counting as described above.

Growth Inhibition Assays

We seeded 1×10^3 exponentially growing COR-L23 cells in 100 μL medium per well into 96-well plates and, after overnight attachment, replaced the medium with that containing 200 nmol/L pemetrexed (a concentration that inhibited growth by ~50%) in the presence or absence of 1 μmol/L thymidine, 10 μmol/L hypoxanthine, and 1% (v/v) DMSO with or without 1 μmol/L inhibitor for 72 h (approximately three cell doubling times). All experiments were conducted in the presence of undialyzed serum as dialysis may remove additional factors required for optimum growth as well as salvageable nucleosides and bases. We fixed the cells and measured growth using the sulforhodamine B assay as described previously (19). The ability to reverse thymidine and hypoxanthine rescue was expressed as a percentage of reversal using the following formula:

% Reversal = 100 × (growth in pemetrexed + thymidine + hypoxanthine − growth in pemetrexed + thymidine + hypoxanthine + inhibitor) ÷ (growth in pemetrexed+thymidine + hypoxanthine − growth in pemetrexed alone).

Tumor Models

All of the *in vivo* experiments were reviewed and approved by the relevant institutional animal welfare committee and done according to the United Kingdom Coordinating Committee on Cancer Research Guidelines for the Welfare of Animals in Experimental Neoplasia (second edition) and national law. We did pharmacokinetic studies in female 8- to 10-wk-old BALB/c mice (Charles River). We determined tissue distribution, pharmacodynamics, and efficacy in female athymic CD1 nude mice (Charles River) implanted with COR-L23 xenografts (1×10^7 cells in 50 μL of PBS injected s.c. into the flank) and maintained and handled in isolators under specific pathogen-free conditions.

Pharmacokinetic Studies

We injected mice with nucleoside transport inhibitors (NU3144, NU3150, NU3151, and NU3153) i.p. at 10 mg/kg in a vehicle of 40% (v/v) polyethylene $glycol_{400}$ in sterile saline. We bled mice by direct cardiac puncture under terminal anesthesia at selected time points after treatment (5–360 min, three mice per time point). Blood was collected into

Published OnlineFirst June 9, 2009; DOI: 10.1158/1535-7163.MCT-08-1208

heparinized tubes and then the plasma was separated and stored at −20°C. We extracted aliquots of plasma (50 μL) with 3 volumes of acetonitrile and applied 50 μL of the supernatant to a 10 × 0.46 cm Genesis C18 4-μm column (Jones Chromatography) fitted with an in-line filter. Compounds were eluted with a mobile phase of 20 mmol/L sodium acetate (pH 5)/acetonitrile at 1 mL/min using a Waters Alliance high-performance liquid chromatography system. Analytes were detected by fluorescence at 450 nm following excitation at 292 nm using a Hewlett-Packard series 1100 fluorescence detector (Agilent Technologies). We determined total (free and protein bound) drug concentrations using linear standard curves (0.05–10 μmol/L; $r^2 > 0.98$ in all cases) generated by extracting compounds from human plasma, with an extraction efficiency of ~100% for all compounds (97–103%), and calculated pharmacokinetic parameters using a noncompartmental model with terminal elimination rate estimated by log-linear regression.

Estimation of Drug Accumulation and [^{3}H]Thymidine Incorporation in Tumors

Experiments commenced when tumors reached an average size of ~0.7 × 0.7 cm (usually ~14 d after implantation). We determined [^{3}H]thymidine incorporation as described previously (16). Briefly, we injected mice (three per group) i.p. with NU3153 (10 mg/kg) or NU3166 (120 mg/kg) and determined [^{3}H]thymidine incorporation 4 and 8 h after a single dose of NU3153 and 8 and 16 h after a second dose given 8 h after the first dose, or 4, 8, 16, 24, and 48 h after a single dose of NU3166 and 24 h after a second NU3166 dose administered 24 h after the first. Forty-five minutes before the end of the experiment, we dosed mice with an i.v. bolus dose of 37 MBq/kg [^{3}H]thymidine (3.7 MBq/mL, 1.78 TBq/mmol, 2.08 μmol/L) in saline via the tail vein. At the end of the experiment, we bled the mice under terminal anesthesia and blood samples were treated as described above. The tumor was removed, placed in foil, frozen in liquid nitrogen, and stored at −80°C before analysis for [^{3}H]thymidine incorporation and determination of drug concentrations. We homogenized the tumor samples in 3 volumes of saline and determined drug levels in 50 μL of homogenate extracted with 19 volumes of acetonitrile, 900 μL of the corresponding supernatant were evaporated to dryness under nitrogen, and samples were reconstituted in 90 μL mobile phase and 50 μL was analyzed by high-performance liquid chromatography as described above. We measured [^{3}H]thymidine incorporation in 500 μL tumor homogenate following precipitation with ice-cold 1 mol/L perchloric acid and subsequent solubilization of the pellet in 1 mL of 1 mol/L NaOH and neutralization with 1 mol/L acetic acid using liquid scintillography by reference to a 20.8 pmol [^{3}H]thymidine standard (1.78 TBq/mmol). Thymidine incorporation was calculated as pmol/g tumor and expressed as a percentage of incorporation into vehicle control tumor samples.

Determination of Antitumor Activity *In vivo*

We treated CD1 nude mice bearing COR-L23 human tumor xenograft (n = 5/group) when tumors were palpable (~0.5 × 0.5 cm, 10–12 d after implantation). We injected mice i.p. with normal saline (control) or pemetrexed, at 1,000 mg/kg/wk for 3 wk in saline, either alone or in combination with 100 mg/kg NU3166 administered i.p. both concomitantly and again 24 h after pemetrexed. Tumor volume was calculated from two-dimensional caliper measurements using the equation $a^2 \times b/2$, where a is the smallest measurement and b the largest. Data are presented as median relative tumor volumes (RTV), where the tumor volume on the initial day of treatment (day 0) is assigned a RTV value of 1 in accordance with the following formula:

RTV = Tumour volume on day of observation/tumour volume on day 0.

Results

Inhibition of Thymidine Transport

Determination of the inhibition of the equilibrative transport of thymidine into L1210 cells by pyrimidopyrimidine nucleoside transport inhibitors at a standard concentration of 1 μmol/L showed that all had equivalent or greater potency than dipyridamole in the absence of AGP. Moreover, whereas the potency of dipyridamole was reduced by 66% in the presence of physiologically relevant concentrations of AGP, AGP had no significant effect on the potency of the novel inhibitors (Fig. 2A).

Our previous studies indicated that inhibition of thymidine transport in L1210 cells correlated with the reversal of thymidine and hypoxanthine rescue in pemetrexed-treated COR-L23 cells (16). However, we wished to investigate if inhibition of thymidine incorporation in COR-L23 cells correlated equally well or better with inhibition of thymidine rescue. We investigated thymidine incorporation in both L1210 cells, as a direct comparison with the thymidine transport assay, and in COR-L23 cells, as a direct comparison with growth inhibition assays. In general, the data obtained at 1 μmol/L inhibitor were similar in all assays and there was no detectable difference in the inhibition of nucleoside incorporation in COR-L23 cells compared with L1210 cells (Table 1). In uptake studies, all of the inhibitors were equivalent to or more potent than dipyridamole at 1 μmol/L and NU3153 was the most potent inhibitor of thymidine incorporation in both cell lines (Supplementary Fig. S1).[3]

Growth Inhibition Assays

The promising potency of the inhibitors in the thymidine transport and incorporation assays led us to investigate their abilities to prevent thymidine and hypoxanthine rescue from pemetrexed-induced growth inhibition. We have previously characterized thymidine and hypoxanthine transport in COR-L23 cells: thymidine uptake, mediated by both ENT1 and ENT2, is inhibited by dipyridamole, but hypoxanthine uptake is insensitive to dipyridamole (20). All compounds, with the exception of NU3144, caused a >100% reversal of thymidine and hypoxanthine rescue in

[3] Supplementary material for this article is available at Molecular Cancer Therapeutics Online (http://mct.aacrjournals.org/).

Published OnlineFirst June 9, 2009; DOI: 10.1158/1535-7163.MCT-08-1208

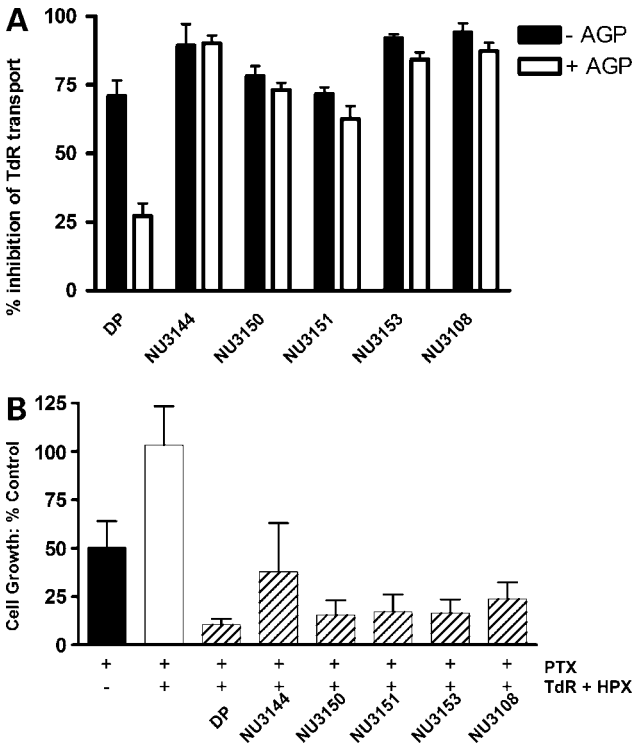

Figure 2. Inhibition of thymidine transport and reversal of pemetrexed-induced growth inhibition. **A,** inhibition of thymidine transport by nucleoside transport inhibitors (1 μmol/L) into L1210 cells in the presence (*white columns*) and absence (*black columns*) of AGP (5 mg/mL). *Columns,* mean of three independent experiments; *bars,* SD. **B,** growth of COR-L23 cells exposed to 200 nmol/L pemetrexed (*PTX*) alone (*black column*) or in combination with 1 μmol/L thymidine (*TdR*) + 10 μmol/L hypoxanthine (*HPX*; *white column*) or in combination with thymidine + hypoxanthine and the inhibitors (*hatched columns*) relative to untreated cells for three cell doubling times. *Columns,* mean of three independent experiments; *bars,* SD.

COR-L23 cells treated with pemetrexed (i.e., growth in the presence of inhibitor and rescue agents was less than that following exposure to pemetrexed alone; Fig. 2B). We presume this was partly due to the presence of thymidine and hypoxanthine in the control medium by virtue of the serum component. Additionally, inhibition of deoxyuridine efflux leading to higher intracellular dUTP, and hence dUTP misincorporation and DNA breaks, as described previously (10), may also contribute to the >100% reversal. NU3144 was significantly less potent than expected from the transport and incorporation data and, on further investigation, was found to be unstable in culture medium (Supplementary Fig. S2).[3]

Plasma Pharmacokinetics

We determined the pharmacokinetics of the lead compounds following an i.p. bolus dose in BALB/c mice. The total plasma concentration time data are shown in Fig. 3A. In all cases, there was evidence of precipitation of compound in the peritoneal cavity at the time of bleeding and this is likely to explain the variability of the data and the lack of first-order pharmacokinetics. NU3144 was not measurable in the plasma. Stability studies confirmed that *in vitro* incubation in control mouse plasma led to breakdown of NU3144 with a half-life of ~24 hours (Supplementary Fig. S2).[3] A total plasma concentration of ≥1 μmol/L, commensurate with that required for inhibition of thymidine incorporation and reversal of thymidine rescue *in vitro*, was only achieved with NU3153 (Fig. 3A). Slow absorption of this compound led to steady state being reached at ~90 minutes, and levels above 1 μmol/L were maintained for at least 6 hours.

Pharmacodynamic Studies with NU3153

Total plasma concentrations of NU3153 were achieved that were predicted, based on *in vitro* data, to be able to inhibit thymidine uptake for at least 6 hours after administration. We therefore investigated the distribution of this compound and inhibition of thymidine incorporation into tumor tissue following administration of 10 mg/kg i.p. as a single dose or as two doses 8 hours apart. Total plasma levels in this study were only 0.5 μmol/L at 4 hours compared with 1.3 μmol/L in the original pharmacokinetic study (Fig. 3A), which may reflect previously observed strain differences (16). Although tumor-associated drug

Table 1. Inhibition of thymidine transport and incorporation in L1210 and COR-L23 cells

	Inhibition of		
	Thymidine transport (L1210)	Thymidine incorporation (L1210)	Thymidine incorporation (COR-L23)
Dipyridamole, 1 μmol/L	80 ± 8%	96 ± 4%	96 ± 1%
Dipyridamole IC_{50}		126 ± 54 nmol/L	15 ± 4 nmol/L
NU3108, 1 μmol/L	83 ± 8%	88%	90 ± 1%
NU3108 IC_{50}		93 nmol/L	26 ± 5 nmol/L
NU3144, 1 μmol/L	98 ± 6%	97%	94%
NU3144 IC_{50}		<10 nmol/L	59 nmol/L
NU3150, 1 μmol/L	93 ± 8%	100%	96%
NU3150 IC_{50}		36.4 nmol/L	60 nmol/L
NU3151, 1 μmol/L	73 ± 6%	100%	93%
NU3151 IC_{50}		41.4 nmol/L	67 nmol/L
NU3153, 1 μmol/L	96 ± 12%	93 ± 4%	96 ± 2%
NU3153 IC_{50}		<10, 43, 8 nmol/L	8 ± 1 nmol/L

NOTE: Data are the mean ± SD of three or more independent experiments or individual experiments. The IC_{50} is the concentration required to inhibit thymidine incorporation by 50% of control.

Published OnlineFirst June 9, 2009; DOI: 10.1158/1535-7163.MCT-08-1208

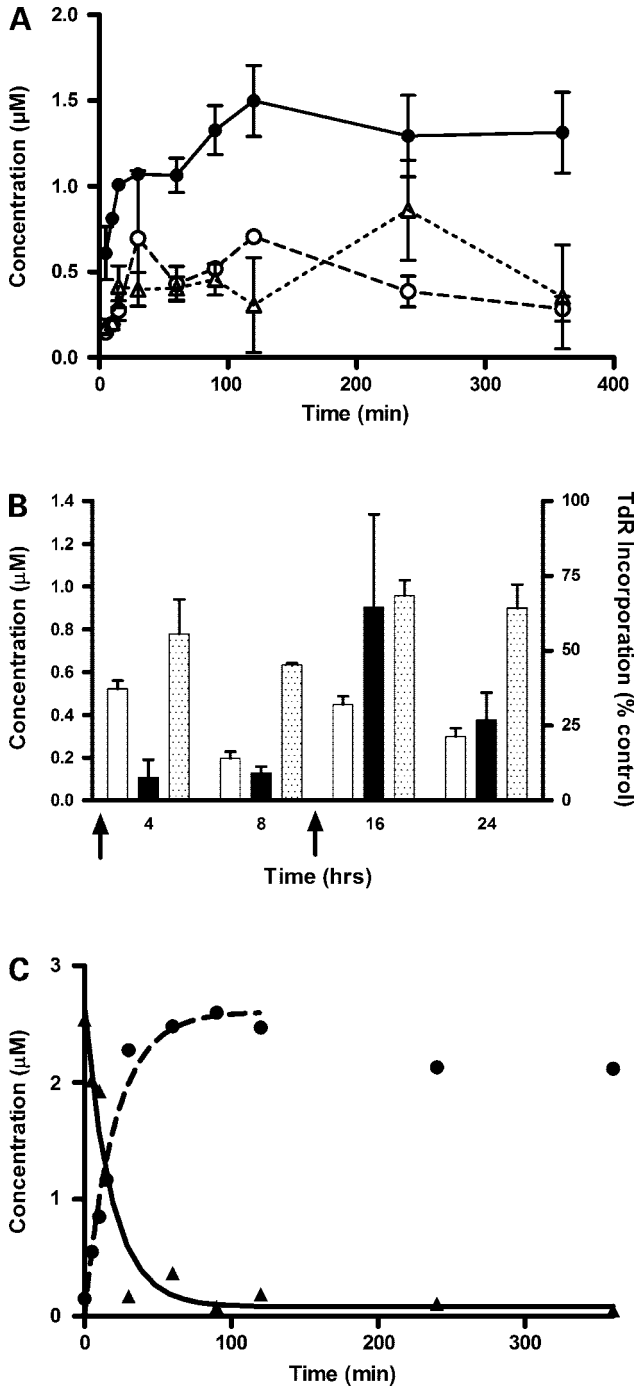

Figure 3. Pharmacokinetics and pharmacodynamics of the nucleoside transport inhibitors. **A,** plasma drug levels in BALB/c mice following i.p. administration of 10 mg/kg NU3150 (○), NU3151 (△), and NU3153 (●). *Points,* mean of three animals per time point for each drug; *bars,* SD. **B,** concentrations of NU3153 in the plasma (*white columns*) and COR-L23 tumor (*black columns*) and the incorporation of thymidine into COR-L23 tumor xenografts (*dotted columns*) at 4, 8, 16, and 24 h after administration of 10 mg/kg NU3153 at 8 hourly intervals. *Arrows,* administration of drug. *Columns,* mean of data from three animals per time point for each drug; *bars,* SD. **C,** *in vitro* breakdown of NU3166 to NU3153 in fresh mouse plasma. Data are from a single representative experiment showing degradation of NU3166 (*triangles, solid line*) and formation of NU3153 (*circles, dashed line*) over time.

levels approached 1 μmol/L 8 hours after the second dose of NU3153, these were not maintained (Fig. 3B).

Inhibition of thymidine incorporation into the tumor was consistent with the lower than expected concentrations of NU3153 detected in plasma and tumor tissue. In control mice, [^{3}H]thymidine incorporation was 1.72 ± 0.64 pmol/g tumor. After a single dose of NU3153, thymidine incorporation into COR-L23 tumors was decreased by 44% to 0.95 ± 0.34 pmol/g at 4 hours and 55% to 0.78 ± 0.02 pmol/g at 8 hours. Eight hours after the second dose, thymidine incorporation was inhibited by 32% to 1.17 ± 0.16 pmol/g. This level of inhibition was maintained such that 16 hours after the second dose thymidine incorporation was still inhibited by 36% relative to control to 1.10 ± 0.23 pmol/g.

Because of the poor aqueous solubility of NU3153, it was not possible to increase the dose of drug to further inhibit thymidine incorporation. We therefore developed a prodrug of NU3153, the valine ester NU3166, to allow higher doses to be administered with the aim of improving both the duration and magnitude of inhibition of thymidine incorporation *in vivo*.

Conversion of Prodrug NU3166 to NU3153 *In vitro*

The valine ester of NU3153, NU3166, was converted rapidly to the parent NU3153 in mouse plasma at 37°C *in vitro*, with a half-life of 14 minutes for liberation of NU3153 and a half-life of 13 minutes for the breakdown of NU3166 as determined by monoexponential kinetics (Fig. 3C).

Inhibition of Thymidine and Hypoxanthine Rescue from Pemetrexed by NU3166

NU3166 inhibited thymidine incorporation into COR-L23 cells by 92 ± 2% at 1 μmol/L and with an IC_{50} of 44 ± 13 nmol/L. The slightly reduced potency of NU3166 compared with the parent compound, NU3153, reflects the rate of breakdown to the active compound, which was found to be complete after 6 hours of incubation in culture medium containing cells. In agreement with this observation, NU3166 prevented the thymidine and hypoxanthine rescue of cells treated with pemetrexed to a similar extent as NU3153 (Supplementary Fig. S3).[3]

Pharmacokinetics of NU3166 and Conversion to NU3153

We determined the pharmacokinetics of NU3166 and NU3153 following both an i.v. and an i.p. bolus dose of NU3166 at 12 mg/kg (equivalent to a 10 mg/kg dose of parent NU3153) in BALB/c mice (Fig. 4A). NU3166 was rapidly converted to NU3153 following administration by either route. As expected, peak levels of both NU3153 and NU3166 were higher and achieved more rapidly following i.v. administration. The pharmacokinetic parameters for NU3153 after i.p. administration of NU3166 were similar to those observed following an i.p. dose of NU3153, with similar peak level of 1.6 and 1.5 μmol/L, and area under the plasma concentration time curve (AUC) values were 378 and 334 μg/mL.min, respectively (Table 2). Administration of NU3166 i.v. resulted in higher peak levels (6.2 μmol/L) and a greater total exposure (AUC of 728 μg/mL.min) to NU3153 than did i.p. administration of either the prodrug or NU3153

Published OnlineFirst June 9, 2009; DOI: 10.1158/1535-7163.MCT-08-1208

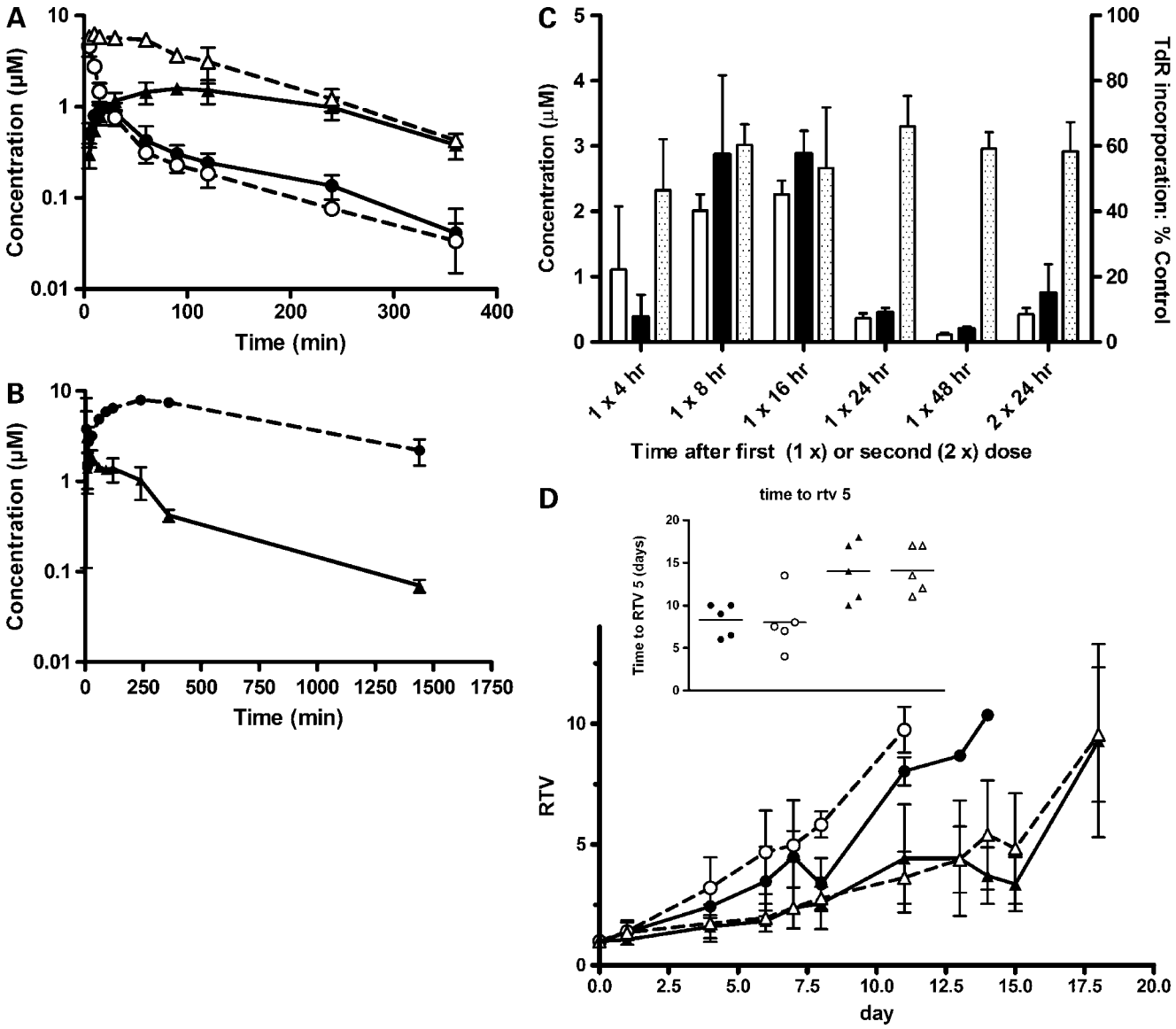

Figure 4. Pharmacokinetics, pharmacodynamics, and efficacy of NU3166. **A,** plasma drug levels of NU3153 (*circles*) and NU3166 (*triangles*) in BALB/c mice following i.p. (*solid symbols, lines*) and i.v. (*open symbols, dashed lines*) administration of 12 mg/kg NU3166. *Points,* mean from three animals per time point for each drug; *bars,* SD. **B,** plasma drug levels of NU3153 (*circles, dashed line*) and NU3166 (*triangles, solid line*) in BALB/c mice following i.p. administration of 120 mg/kg NU3166. *Points,* mean from three animals per time point; *bars,* SD. **C,** concentrations of NU3153 in the plasma (*white columns*) and tumor (*black columns*) and the incorporation of thymidine into tumor xenografts (*dotted columns*) at intervals following either a single dose (*1*×) or two doses at 24-h intervals (*2*×) of 120 mg/kg NU3166 administered i.p. *Columns,* mean from three animals per time point; *bars,* SD. **D,** effects of NU3153 on pemetrexed efficacy *in vivo*. Growth of COR-L23 tumor xenografts, following daily treatment with vehicle control alone (●), NU3166 alone given weekly on 2 d (120 mg/kg, days 0 and 1, 6 and 7, and 13 and 14; ○), pemetrexed alone given weekly (1,000 mg/kg, days 0, 6, and 13; ▲), or NU3166 weekly on 2 d (120 mg/kg) and pemetrexed weekly (1,000 mg/kg; △). For all experiments, tumor size is presented as the median tumor volume of surviving mice, measured relative to tumor volumes on day 0 (based on five animals per group). *Inset,* time to RTV 5 for individual mice. *Horizontal bar,* mean.

itself. The half-life of NU3153 following either i.v. (84 minutes) or i.p. (120 minutes) administration of the prodrug NU3166 was ~10 times shorter than following i.p. administration of NU3153. Thus, by overcoming the problems of water solubility and the associated peritoneal precipitation, the drug was no longer maintained at the concentrations required for inhibition of thymidine incorporation following a dose of 12 mg/kg.

Increasing the dose of NU3166 to 120 mg/kg i.p. was well tolerated. However, there was a suggestion of nonlinearity of the pharmacokinetics of NU3153 with the apparent clearance of NU3153 being approximately half that seen at 12 mg/kg with a commensurate ~20-fold increase in AUC. In addition, plasma levels of the parent NU3153 were 2.2 ± 0.7 μmol/L at 24 hours (Fig. 4B), well above the 1 μmol/L target concentration required for *in vitro* inhibition of thymidine incorporation.

Published OnlineFirst June 9, 2009; DOI: 10.1158/1535-7163.MCT-08-1208

Table 2. Plasma pharmacokinetic parameters for NU3166 and NU3153 following either a single dose of NU3153 at 10 mg/kg i.p., NU3166 at 12 mg/kg i.p. or i.v., or 120 mg/kg i.p.

Drug and dose	NU3153, 10 mg/kg i.p.	NU3166, 12 mg/kg (≡10 mg/kg NU3153) i.p.		NU3166, 12 mg/kg (≡10 mg/kg NU3153) i.v.		NU3166, 120 mg/kg (≡100 mg/kg NU3153) i.p.	
Compound detected	NU3153	NU3166	NU3153	NU3166	NU3153	NU3166	NU3153
AUC (μg/mL.min)	334	82	378	95	728	587	6,933
Clearance (mL/min/kg)	4.8	122	27	106	14	170	14
Half-life (min)	1259	97	120	95	84	307	634
C_{max} (μmol/L)	1.5	0.9	1.6	4.6	6.2	3.0	7.9
T_{max} (min)	120	15	90	5	10	5	240
Time above 1 μmol/L (min)	>345<1,440	n/a	210	15	>240<360	120	>1,440
V_{dss} (L/kg)	0.15	11	3.5	6.2	1.4	46	5.5

Distribution of NU3166/NU3153 to the Tumor and Inhibition of Thymidine Incorporation

We measured the total plasma and tumor concentrations of NU3153 at various times after a single dose or two doses of 120 mg/kg NU3166, administered 24 hours apart (Fig. 4C). Peak concentrations were seen at 16 hours in both plasma (2.3 ± 0.2 μmol/L) and tumor (2.9 ± 0.4 μmol/L). Plasma concentrations of NU3153 in CD1 nude mice were again lower than predicted from the pharmacokinetic study in BALB/c mice, assuming linear pharmacokinetics, although the 24-hour time point was the only directly comparable time point (0.36 ± 0.08 μmol/L in CD1 versus 2.2 ± 0.71 μmol/L in BALB/c). Nevertheless, the tumor-associated concentrations of NU3153 were >1 μmol/L for at least 16 hours in CD1 mice.

In parallel, we measured the ability of NU3166 to inhibit thymidine incorporation into COR-L23 tumor xenografts (Fig. 4C). In control untreated mice, [^{3}H]thymidine incorporation was 0.66 ± 0.01 pmol/g tumor. Thymidine incorporation was inhibited by 35% to 55% for up to 48 hours following either one or two doses of NU3166, less inhibition than expected based on the tumor NU3153 concentrations.

Antitumor Activity of NU3166 in Combination with Pemetrexed

The higher tumor-associated concentrations of NU3153 achievable with prodrug administration facilitated a study to investigate the enhancement of pemetrexed activity by NU3166. Control COR-L23 xenografts grew rapidly, reaching a median RTV of 5 by 9 days, and NU3166 alone did not significantly affect tumor growth (time to RTV 5 = 7.5 days; P = 0.8, Mann-Whitney). Pemetrexed extended the time taken to reach RTV 5 to 14 days (5-day growth delay; P = 0.016). The combination also significantly increased time to RTV 5 (13.5 days) compared with saline-treated controls (P = 0.008); however, this growth delay was not significantly different from pemetrexed alone (P = 1.00; Fig. 4D). These data suggest that although high concentrations of NU3153 can be achieved in the tumor, the lack of improvement in pemetrexed efficacy is due to the modest inhibition of thymidine incorporation.

Discussion

The aim of the study reported here was to determine the biological activity of novel pyrimidopyrimidine nucleoside transport inhibitors derived from dipyridamole and to assess their ability to inhibit thymidine uptake and enhance antifolate antitumor activity *in vitro* and *in vivo*. At a fixed concentration of 1 μmol/L, all analogues were approximately equally potent inhibitors of thymidine transport compared with dipyridamole. Importantly, unlike dipyridamole, none of the analogues showed a reduction in potency in the presence of AGP.

In our previous investigations of nucleoside transport inhibitors, we had used a rapid (12 seconds) inhibitor-stop assay that, although it measured initial rates of equilibrative transport (21), was technically challenging, required large amounts of cells and radiolabel, and produced a significant quantity of solid radioactive waste. We therefore investigated whether measuring thymidine incorporation over a 2-hour period might be an equally reliable and simpler assay. Both methods were compared in L1210 cells, and the data were broadly similar in both assays. When these data were compared with the ability of the compounds to reverse thymidine and hypoxanthine rescue of COR-L23 cells from pemetrexed-induced growth inhibition, there was slightly greater concordance with the thymidine incorporation data. We therefore believe that thymidine incorporation represents a simpler, less hazardous assay that is, if anything, a more reliable indicator of antiproliferative activity. It is possible that the high concentrations of thymidine needed to drive the transport assay force an abnormal nonphysiologic concentration gradient that would be toxic to long-term cultures and do not reflect the normal functioning of the transporters.

Complete reversal of thymidine and hypoxanthine rescue from pemetrexed-induced growth inhibition was achieved with all analogues. However, none of the analogues was as efficient as dipyridamole. This suggests that dipyridamole may have additional properties over and above its ability to inhibit nucleoside transport such as the ability to inhibit some of the drug efflux pumps, including ABCB1 (MDR1; refs. 9, 22), ABCC1 (MRP1; ref. 23), and ABCG2 (BCRP), which can transport antifolates (24, 25). The present study focused on inhibition of nucleoside transport as a strategy to improve antifolate activity, and it is not known if the novel analogues affect antifolate efflux and hence the intracellular concentration of pemetrexed.

Published OnlineFirst June 9, 2009; DOI: 10.1158/1535-7163.MCT-08-1208

A concentration of 1 μmol/L of each of the inhibitors was required to inhibit rescue from pemetrexed-induced growth inhibition by 1 μmol/L thymidine in COR-L23 cells. This concentration of thymidine was selected as being similar to those observed in mice (26). In cancer patients, plasma thymidine concentrations have been reported to be in the range of 50 to 900 nmol/L, although a recent publication suggests they are closer to 12 nmol/L (27). Because the concentration of thymidine in mouse plasma is 1 μmol/L (26), it was anticipated that plasma levels of the inhibitors would have to be maintained at concentrations ≥1 μmol/L to inhibit thymidine uptake into mice bearing human tumor xenografts. Only NU3153 showed an acceptable pharmacokinetic profile, although limited solubility led to precipitation of the compound at the injection site, thereby limiting the maximum dose administrable. Interestingly, there seemed to be a difference in the pharmacokinetics of NU3153 between the two strains of mice used in these experiments. Although total plasma levels of NU3153 were in excess of 1 μmol/L for at least the first 6 hours in BALB/c mice, levels achieved in tumor-bearing CD1 *nu/nu* mice were 0.5 μmol/L or less and tumor-associated concentrations of NU3153 approaching those needed for *in vitro* rescue inhibition were only observed up to 16 hours. As a consequence, [^{3}H]thymidine incorporation into COR-L23 xenografts was only inhibited by up to 50% over a 24-hour period. Curiously, inhibition of thymidine incorporation remained at a more-or-less constant level of 40% to 50% irrespective of the tumor-associated concentration of NU3153.

The development of a prodrug of NU3153, with equivalent *in vitro* rescue inhibitory activity to the parent compound and improved aqueous solubility, allowed a much higher dose to be administered. The compound was rapidly converted into the parent compound, and there was a consequent increase in both the total plasma and tumor-associated concentrations of NU3153 and hence the time above the 1 μmol/L threshold. As observed in the previous pharmacodynamic experiment, there was an apparent difference in the two strains of mice, with lower levels of NU3153 being observed in the tumor-bearing CD1 *nu/nu* mice. Nevertheless, total plasma and tumor-associated levels of NU3153 were above 1 μmol/L for at least the first 16 hours. Unfortunately, these concentrations of NU3153 did not translate into an improved ability to inhibit thymidine incorporation into COR-L23 xenografts, which remained around 40% to 50% as in the previous study. This result was disappointing as *in vitro* studies suggested that thymidine uptake needed to be inhibited by ≥90% to prevent thymidine rescue from pemetrexed cytotoxicity. Thus, it would appear from our studies that 50% inhibition of thymidine incorporation is the maximum achievable using the approach studied here. This may be due to the tumor architecture, hemodynamics, or potential binding of NU3153 to stromal proteins. Consistent with the failure to inhibit thymidine incorporation by ≥90%, NU3166 failed to improve the efficacy of pemetrexed in the COR-L23 human tumor xenograft model. Although pemetrexed was administered as a single dose at weekly intervals, it is likely to persist in the tumor cells due to polyglutamation, which increases its activity against the target enzymes and retention within the target cell. Had NU3166 been given on a daily basis, persistent inhibition of thymidine incorporation may have afforded some additional activity. However, alternative schedules have not been investigated.

In conclusion, we have developed novel potent nucleoside transport inhibitors that overcome the AGP binding that limits the clinical efficacy of dipyridamole. These analogues show promising activity in *in vitro* studies. The development of a prodrug (NU3166) of the compound with the best pharmacokinetic profile allowed the administration of a dose that produced and maintained concentrations of drug NU3153 that were consistent with *in vitro* activity. However, inhibition of thymidine incorporation into the tumor was not sufficient to lead to an increase in the efficacy of the antifolate pemetrexed in a COR-L23 human tumor xenograft model. Clearly, improvements in the pharmacologic properties, or alternative schedules of administration, will be necessary to translate the promising "proof of principle" *in vitro* data into equally promising preclinical data that would justify the initiation of clinical studies.

Disclosure of Potential Conflicts of Interest

D.R. Newell, R.J. Griffin, B.T. Golding, and N.J. Curtin: inventors on patents relating to these compounds. No other potential conflicts of interest were disclosed.

References

1. Walling J. From methotrexate to pemetrexed and beyond. A review of the pharmacodynamics and clinical properties of antifolates. Invest New Drugs 2006;24:37–77.

2. Weber G. Biochemical strategy of cancer cells an the design of chemotherapy: G. H. A. Clowes Memorial Lecture. Cancer Res 1983;43:3466–92.

3. Kinsella AR, Harran MS. Decreasing sensitivity to cytotoxic agents parallels increasing tumorigenicity in human fibroblasts. Cancer Res 1991;51:1855–9.

4. Webber S, Bartlett CA, Boritzki TJ, et al. AG337, a novel lipophilic thymidylate synthase inhibitor: *in vitro* and preclinical studies. Cancer Chemother Pharmacol 1996;37:509–17.

5. Worzalla JF, Shih C, Schultz RM. Role of folic acid in modulating the toxicity and efficacy of the multitargeted antifolate LY231514. Anticancer Res 1998;18:3235–40.

6. Schultz RM, Patel VF, Worzalla JF, Shih C. Role of thymidylate synthase in the antitumour activity of the multitargeted antifolate LY231514. Anticancer Res 1999;19:437–44.

7. Baldwin SA, Mackey JR, Cass CE, Young JD. Nucleoside transporters: molecular biology and implications for therapeutic development. Mol Med Today 1999;5:216–24.

8. Schaper W. Dipyridamole, an underestimated vascular protective drug. Cardiovasc Drugs Ther 2005;19:357–63.

9. Goel R, Howell SB. Modulation of the activity of cancer chemotherapeutic agents by dipyridamole. In: Muggia FM, editor. New drugs, concepts and results in cancer chemotherapy. Boston: Kluwer Academic Publishers 1992; 19–44.

10. Curtin NJ, Harris AL, Aherne GW. Mechanism of cell death following thymidylate synthase inhibition: 2′-deoxyuridine-5′-triphosphate accumulation, DNA damage and growth inhibition following exposure to CB3717 and dipyridamole. Cancer Res 1991;51:2346–52.

11. Curtin NJ, Newell DR, Harris AL. Modulation of dipyridamole action by α1 acid glycoprotein. Reduced potentiation of quinazoline antifolate (CB3717) cytotoxicity by dipyridamole. Biochem Pharmacol 1989;38:3281–8.

12. Willson JKV, Fischer PH, Remick SC, et al. Methotrexate and

Published OnlineFirst June 9, 2009; DOI: 10.1158/1535-7163.MCT-08-1208

dipyridamole combination chemotherapy based upon inhibition of nucleoside salvage in humans. Cancer Res 1988;48:5585–90.

13. Budd GT, Jayaraj A, Grabowski D, et al. Phase I trial of dipyridamole with 5-fluorouracil and folinic acid. Cancer Res 1990;50:7206–11.

14. Curtin NJ, Bowman KJ, Turner RN, et al. Potentiation of the cytotoxicity of thymidylate synthase (TS) inhibitors by dipyridamole analogues with reduced α_1-acid glycoprotein binding. Br J Cancer 1999;80:1738–46.

15. Curtin NJ, Barlow HC, Bowman KJ, et al. Resistance-modifying agents. 11. Pyrimido[5,4-*d*]pyrimidine modulators of antitumor drug activity. Synthesis and structure-activity relationships for nucleoside transport inhibition and binding to α_1-acid glycoprotein. Journal of Medicinal Chemistry 2004;47:4905–22.

16. Smith PG, Thomas HD, Barlow HC, et al. *In vitro* and *in vivo* properties of novel nucleoside transport inhibitors with improved pharmacological properties that potentiate antifolate activity. Clin Cancer Res 2001;7:2105–13.

17. Smith PJ, Marshman E, Newell DR, Curtin NJ. Dipyridamole potentiates the *in vitro* activity of MTA (LY231514) by inhibition of thymidine transport. Br J Cancer 2000;82:924–30.

18. Curtin NJ, Harris AL. Potentiation of quinazoline antifolate (CB3717) toxicity by dipyridamole in A549 cells. Biochem Pharmacol 1998;37:2113–20.

19. Skehan P, Storeng R, Scudiero D, et al. New colorimetric cytotoxicity assay for anticancer-drug screening. J Natl Cancer Inst 1990;82:110–2.

20. Marshman E, Taylor GA, Thomas HD, Newell DR, Curtin NJ. Hypoxanthine transport in human tumour cell lines. Relationship to the inhibition of hypoxanthine rescue by dipyridamole. Biochem Pharmacol 2001;61:477–84.

21. Wohlhueter RM, Marz R, Graff JC, Plagemann PGW. A rapid-mixing technique to measure transport in suspended animal cells: applications to nucleoside transport in Novikoff rat hepatoma cells. Methods Cell Biol 1978;20:211–36.

22. Asoh K-I, Yoshio S, Sato S-I, Nogae I, Kohno K, Kuwano M. Potentiation of some anticancer agents by dipyridamole against drug-sensitive and drug-resistant cancer cell lines. Jpn J Cancer Res 1990;80:475–81.

23. Curtin NJ, Turner DP. Dipyridamole-mediated reversal of multidrug resistance in MRP over-expressing human lung carcinoma cells *in vitro*. Eur J Cancer 1999;35:1020–6.

24. Polgar O, Robey RW, Bates SE. ABCG2: structure, function and role in drug response. Expert Opin Drug Metabol Toxicol 2008;4:1–5.

25. Worm J, Kirkin AF, Dzhandzhugazyan KN, Guldberg P. Methylation-dependent silencing of the reduced folate carrier gene in inherently methotrexate-resistant human breast cancer cells. J Biol Chem 2001;276:39990–40000.

26. Jackman AL, Taylor GA, Calvert AH, Harrap KR. Modulation of antimetabolite effects: effects of thymidine on the efficacy of the quinazoline-based thymidylate synthetase inhibitor, CB3717. Biochem Pharmacol 1984;33:3269–75.

27. Li KM, Rivory LP, Hoskins J, Sharma R, Clarke SJ. Altered deoxyuridine and thymidine in plasma following capecitabine treatment in colorectal cancer patients. Br J Clin Pharmacol 2006;63:67–74.

AACR American Association for Cancer Research

Molecular Cancer Therapeutics

Preclinical evaluation of a novel pyrimidopyrimidine for the prevention of nucleoside and nucleobase reversal of antifolate cytotoxicity

Huw D. Thomas, Kappusamy Saravanan, Lan-Zhen Wang, et al.

Mol Cancer Ther 2009;8:1828-1837. Published OnlineFirst June 9, 2009.